



Published in final edited form as:

Dev Cell. 2016 December 19; 39(6): 683–695. doi:10.1016/j.devcel.2016.11.015.

Slit-Robo Repulsive Signaling Extrudes Tumorigenic Cells from Epithelia

John Vaughen¹ and Tatsushi Igaki^{1,2,*}

¹Laboratory of Genetics, Graduate School of Biostudies, Kyoto University, Yoshida-Konoecho, Sakyo-ku, Kyoto 606-8501, Japan

²Lead Contact

SUMMARY

Cells dynamically interact throughout animal development to coordinate growth and deter disease. For example, cell-cell competition weeds out aberrant cells to enforce homeostasis. In *Drosophila*, tumorigenic cells mutant for the cell polarity gene *scribble* (*scrib*) are actively eliminated from epithelia when surrounded by wild-type cells. While *scrib* cell elimination depends critically on JNK signaling, JNK-dependent cell death cannot sufficiently explain *scrib* cell extirpation. Thus, how JNK executed cell elimination remained elusive. Here, we show that repulsive Slit-Robo2-Ena signaling exerts an extrusive force downstream of JNK to eliminate *scrib* cells from epithelia by disrupting E-cadherin. While loss of Slit-Robo2-Ena in *scrib* cells potentiates *scrib* tumor formation within the epithelium, Robo2-Ena hyperactivation surprisingly triggers luminal *scrib* tumor growth following excess extrusion. This extrusive signaling is amplified by a positive feedback loop between Slit-Robo2-Ena and JNK. Our observations provide a potential causal mechanism for Slit-Robo dysregulation in numerous human cancers.

Graphical Abstract

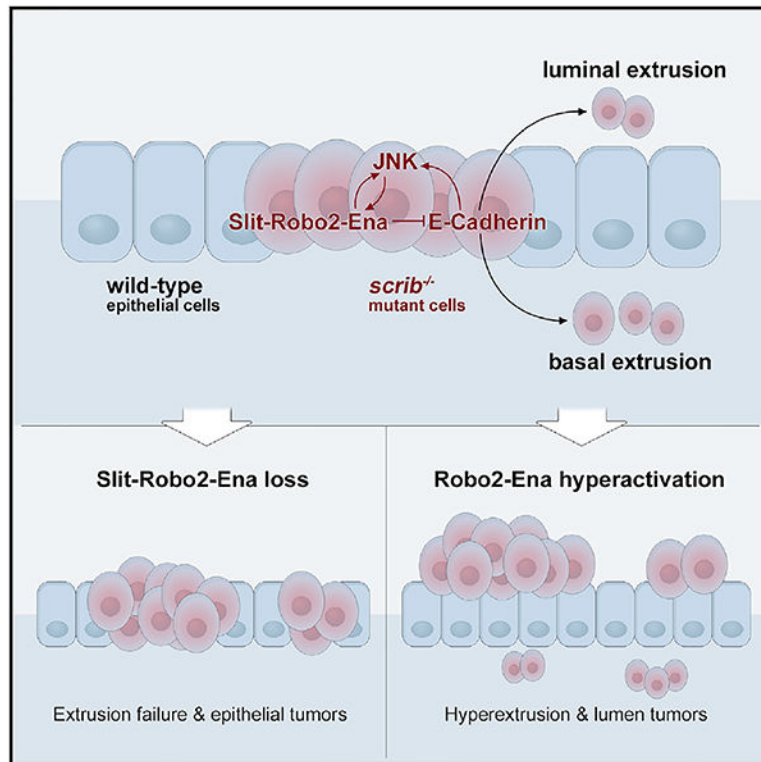
*Correspondence: igaki@lif.kyoto-u.ac.jp.

AUTHOR CONTRIBUTIONS

T.I. designed the screen; J.V. designed and conducted all subsequent experiments with input from T.I.; J.V. analyzed the data with input from T.I.; J.V. and T.I. wrote the manuscript.

SUPPLEMENTAL INFORMATION

Supplemental Information includes Supplemental Experimental Procedures and six figures and can be found with this article online at <http://dx.doi.org/10.1016/j.devcel.2016.11.015>.



In Brief

Tumor-suppressive programs remove aberrant cells from developing tissues. Vaughen and Igaki identify Slit-Robo2-Ena as the extrusive force behind polarity-deficient cell elimination from *Drosophila* epithelia. While loss of Slit-Robo2-Ena permits tumor formation within the epithelium, Slit-Robo2-Ena signaling hyperactivation triggers excess extrusion and luminal tumor overgrowth.

INTRODUCTION

Cell-cell interactions suppress tumorigenesis by eliminating weak or aberrant cells from tissues in a conserved process called cell competition (reviewed in Tamori and Deng, 2011; de Beco et al., 2012; Levayer and Moreno, 2013; Amoyel and Bach, 2014; Morata and Ballesteros-Arias, 2015). One example of tumor-suppressive cell competition is the active removal of cells lacking *scribble* (*scrib*) or *discs large* (*dlg*), evolutionarily conserved apicobasal polarity genes (Brumby and Richardson, 2003; Igaki et al., 2009). It was previously reported that c-Jun N-terminal kinase (JNK) signaling has critical autonomous and non-autonomous roles in *scrib* cell elimination (Brumby and Richardson, 2003; Igaki et al., 2009; Ohsawa et al., 2011), with non-autonomous JNK promoting wild-type neighbors to engulf *scrib* cells (Ohsawa et al., 2011). However, autonomous JNK's function in *scrib* cell elimination was less clear, as merely blocking cell death does not cause as drastic tumorigenesis as blocking JNK (Brumby and Richardson, 2003). Thus, key downstream mechanisms of tumor-suppressive JNK signaling in *scrib* cell elimination remained unknown.

Here we identify novel JNK targets crucial for *scrib* cell elimination: the ligand Slit, its transmembrane Roundabout receptor Robo2, and the downstream cytoskeletal effector Enabled/VASP (Ena). The Slit-Robo system is a conserved axon-guidance module that controls cell repulsion and migration (Brose and Tessier-Lavigne, 2000; Araújo and Tear, 2003). Classically, Robo receptors expressed on migrating axons bind to Slit secreted from midline glia, repelling axons in a dynamic process dependent on Ena (Kidd et al., 1999; Brose et al., 1999; Bashaw et al., 2000; Simpson et al., 2000a, 2000b; Rajagopalan et al., 2000). Recent studies, however, have uncovered unconventional Slit-Robo signaling in muscle-tendon guidance (Ordan and Volk, 2015), intestinal stem cell control (Biteau and Jasper, 2014), germline stem cell competition (Stine et al., 2014), and foregut separation (Domyan et al., 2013). Our present study reveals an important role for Slit-Robo in extruding tumorigenic cells from epithelia through E-cadherin (E-cad) deregulation. While JNK-activated Slit-Robo2-Ena extrudes *scrib* cells and thus functions as a tumor suppressor, signal hyperactivation can also promote tumorigenesis by increased luminal extrusion. Our data help to explain how Slit-Robo signaling acts as both a tumor suppressor and tumor promoter in human cancers.

RESULTS

Slit-Robo2-Ena Signaling Is Required for Scrib Cell Elimination

Tumorigenic cell clones mutant for *scrib* are eliminated from *Drosophila* eye imaginal epithelium. To gain insight into factors regulating *scrib* cell elimination, we conducted a genetic screen in *Drosophila* eye discs by introducing a series of heterozygous chromosomal deficiencies into the *scrib* mosaic background and screening for aberrant *scrib* cell overgrowth (Figure S1A). We recovered many deficiency hits that permitted *scrib* cell overgrowth (J.V. and T.I., unpublished data). Two such overlapping deficiencies uncovered the actin nucleator Enabled/VASP (Ena), which we identified as essential for *scrib* cell elimination (Figures S1B–S1F). While GFP-labeled *scrib* clones are eliminated and only contribute to 10% of eye discs compared with 35% for control clones (Figures 1A and 1B), heterozygosity for an *ena* null allele, *ena*²³ (Ahern-Djamali et al., 1998), doubled *scrib* clone size (Figure 1C, quantified in Figure 1I). As Ena acts downstream of Slit-Robo in *Drosophila* (Bashaw et al., 2000) and *Caenorhabditis elegans* (Yu et al., 2002), we next tested these candidate upstream axon-guidance signals. Intriguingly, heterozygosity for the ligand *slit* or its receptor *robo2* also caused significant *scrib* clone overgrowth (Figures 1D, 1E, S1M, and S1N). Heterozygosity for *robo1* and *robo3* did not alter *scrib* clone size (Figures S1K and S1L), suggesting that Robo2 has a specific role in *scrib* cell elimination.

To next test whether Slit-Robo2-Ena functions in *scrib* clones or surrounding wild-type cells, we depleted each protein in only *scrib* or wild-type cells using *RNAi*. While Slit-Robo knockdown in wild-type cells surrounding *scrib* mutant cells did not induce overgrowth (data not shown), knockdown specifically within *scrib* clones potentiated strong overgrowth (Figures 1F–1H and S1Q). Knockdown of Slit, Robo2, or Ena alone in clones did not alter tissue growth (Figures S1G–S1J, quantified in Figure S1S). Neither *robo1-RNAi* nor *robo3-RNAi* affected *scrib* cell elimination (Figures S1O and S1P), whereas total Robo downregulation via overexpression of Commissureless (Comm) (Keleman et al., 2002)

phenocopied *robo2-RNAi*-induced *scrib* clone overgrowth (Figure S1R). These results suggest that Slit-Robo2-Ena signaling is specifically required within *scrib* cells to eliminate *scrib* cells from epithelia.

Slit, Robo2, and Ena Are Upregulated in Scrib Clones

We next examined the expression patterns of Slit, Robo2, and Ena in *scrib* mosaic tissue. *Slit* transcription was markedly increased in *scrib* clones compared with wild-type eye disc cells (Figures 2A–2B', quantified in Figure 2G; compare with Figures S2A–S2B', note endogenous *slit* transcription [asterisk] in the peripodial epithelium). Slit protein also accumulated in *scrib* clones (Figures S2G–S2G''). To evaluate Robo2 expression, we employed a hemagglutinin (HA)-tagged Robo2 knockin into the endogenous Robo2 locus (*robo2^{HA-robo2}*), which is expressed identically to wild-type Robo2 protein (Spitzweck et al., 2010). While endogenous Robo2 expression was scarce in wild-type discs (Figures S2C–S2D'), *scrib* clones strongly upregulated Robo2 (Figures 2C–2D'). In contrast, Robo1 and Robo3 were not specifically upregulated within *scrib* clones (data not shown). In addition, Ena accumulated cell-autonomously in *scrib* cells compared with wild-type neighbors (Figures 2E–2F', arrowheads; compare with Figures S2E–S2F'). Thus, Slit, Robo2, and Ena are upregulated in *scrib* clones.

Further confirming Slit-Robo activation within *scrib*, removal of surrounding wild-type tissue through overexpression of a proapoptotic gene (Stowers and Schwarz, 1999) revealed strong JNK and *slit-lacZ* activation still present in *scrib* eye discs (Figures S2H–S2J'). Thus, while Slit-Robo and JNK signaling affect cell competition, autonomous activation of these pathways is not dependent on the presence of wild-type cells, which instead contribute to *scrib* engulfment (Ohsawa et al., 2011). Notably, though in the above localization experiments we overexpressed caspase-inhibitor p35 within *scrib* clones to increase clone size, we still observed Slit-Robo2-Ena upregulation within certain plain *scrib* clones (Figures S2K–S2L' and data not shown). This also indicates that Slit-Robo2-Ena upregulation is not merely the result of apoptosis. Taken together with the *RNAi* experiments, these data support that autocrine Slit-Robo2-Ena activation mediates *scrib* cell elimination.

Slit-Robo2-Ena Signaling Acts Downstream of JNK Signaling in Scrib Cell Elimination

We next investigated how Slit-Robo2-Ena signaling was upregulated in *scrib* clones. As JNK signaling is critical for *scrib* cell elimination, we reasoned that JNK may also be essential for Slit-Robo2-Ena upregulation. Strikingly, in *scrib* clones with impaired JNK signaling (by a dominant-negative form of the *Drosophila* JNK Basket, *bsk^{DN}*), *slit* transcription and Robo2-Ena upregulation were completely abrogated (Figures 3A–3F', compare with Figures 2A–2F'). Moreover, JNK activation by over-expression of a constitutively active form of the JNK kinase Hemipterous (*hep^{CA}*) was sufficient to upregulate Robo2 (Figures 3G–3H'', MMP1 is a JNK-target gene), Ena (Figures 3I and 3J), and *slit* transcription (Figures 3I'–3J''). Supporting JNK-dependent activation of Slit-Robo2-Ena, we found multiple AP1 consensus sequences (TGA(G/C)TCA; Angel et al., 1987) within introns of all three genes (Figure S3). Slit contains six AP1 consensus sequences, two of which precede a

transcriptional start site (Figure S3A); Robo2 only contains three AP1 consensus sequences (Figure S3B), which may explain its weaker upregulation by JNK.

If Slit-Robo2-Ena functionally act downstream of JNK during *scrib* cell elimination, Slit-Robo2-Ena overexpression in JNK-deficient *scrib* clones should prevent overgrowth. Indeed, although *scrib + bsk^{DN}* clones massively overgrow (Figure 3K), co-expression of Slit, Robo2, or Ena (Figures 3L–3N) significantly reduced *scrib + bsk^{DN}* overgrowth by ~50% (Figure 3O). These data place Slit-Robo2-Ena downstream of JNK signaling in *scrib* cell elimination.

Slit-Robo2-Ena Signaling Mediates Scrib Cell Extrusion

We next sought to understand how Slit-Robo2-Ena signaling eliminates *scrib* cells. In the course of the above experiments, we observed that *scrib* cells were often not located in the main epithelium (disc proper, DP) but instead were extruding basally (orange asterisks, Figures 4A and 4B) or into the lumen (blue asterisks, Figures 4A and 4B). While cell extrusion is a central mechanism for enforcing cell competition in mammalian cell culture systems (Hogan et al., 2009), certain in vivo studies have suggested that extrusion passively follows cell death (Lolo et al., 2012; Levayer et al., 2016). We therefore tested the effect of caspase inhibition on *scrib* cell extrusion and found that extrusion still occurred: large masses of basally extruding *scrib* cells were displaced away from the DP (Figure 4C, quantified in Figure 4M). This suggests that basal *scrib* cell extrusion occurs prior to cell death, which is consistent with prior findings using *scrib-RNAi* and caspase inhibition (Nakajima et al., 2013). Moreover, we infer that basal extrusion is rapidly followed by cell death, as the number of observed extruding cells nearly doubled upon caspase inhibition (Figure 4M).

Because Slit-Robo signaling is canonically repulsive, we hypothesized that Slit-Robo2-Ena could regulate the extrusion of *scrib* cells. Indeed, knockdown of Slit, Robo2, or Ena abrogated apical/basal extrusion of *scrib* cells, with resultant *scrib* tumors accumulating in the DP (Figures 4D–4F, quantified in Figure 4M). A similar result was obtained for heterozygous alleles of *slit*, *robo2*, or *ena* (Figures S4A–S4C, quantified in Figure S4H). Moreover, JNK inhibition also strongly suppressed *scrib* cell extrusion (Figure S4D). Conversely, Slit-Robo2-Ena overexpression dramatically evicted nearly all *scrib* cells from the DP, with the vast majority of surviving *scrib* clones located in the lumen (Figures 4G–4I, blue asterisks). However, blocking cell death in Slit-Robo2-Ena-overexpressing *scrib* cells again revealed many basally extruding populations (Figures 4J–4L, orange asterisks). Slit-Robo2-Ena therefore extrudes *scrib* cells from the DP in a directionally unbiased manner (basally or luminally), and the apparent bias toward lumen clones upon Slit-Robo2-Ena hyperactivation derives from the rapid death of basally extruded cells. Importantly, we observed cases of Slit-Robo pathway activation prior to cell extrusion (arrows in Figures S2L–S2L' and data not shown), suggesting that pathway activation precedes extrusion.

In support of Slit-Robo2-Ena executing cell extrusion downstream of JNK, Slit-Robo2-Ena co-expression in JNK-deficient *scrib* cells partially rescued extrusion (Figures S4E–S4G, compare with Figure S4D, quantified in Figure S4H), consistent with Slit-Robo2-Ena co-expression partially reducing JNK-deficient *scrib* tumor size (Figures 3K–3O).

Robo2-Ena Hyperactivation Triggers *Scrib* Tumorigenesis in the Lumen

While basally extruded *scrib* cells seemed to be removed rapidly via apoptosis (Figures S4I and S4J), luminal *scrib* cells were not universally dying (Figures S4K and S4L). Instead, upon Robo2 or Ena overexpression in *scrib* clones, luminal *scrib* clones over-grew into significant tumors (Figures 4N–4Q, quantified in Figure 4R). This is not trivially due to Robo2 or Ena overexpression alone, as Robo2- or Ena-overexpressing clones were actually smaller than wild-type clones (Figures S4M–S4Q, quantified in Figure S4R) and frequently underwent basal apoptosis (Figures S4S–S4T'). Although lumen tumor overgrowth was also observed in Slit-overexpressing *scrib* clones (Figures S4U and S4V), luminal tumors were rarer than in Robo2- or Ena-overexpression conditions. Notably, Slit overexpression in *scrib* cells caused a weaker increase in luminal extrusion compared with Robo2 or Ena overexpression in *scrib* (Figure 4M), suggesting a functional link between extrusion strength and luminal tumors. The differences between Slit and Robo2/Ena overexpression likely reflect a difference in the strength of signal activation between ligand overexpression and downstream component (Robo2-Ena) overexpression. Importantly, the Slit-overexpression transgene yielded stronger Slit upregulation than Robo2 overexpression (Figures S4W–S4W'', compare with Figures S4X–S4X''), suggesting that the different outcomes between Slit and Robo2 overexpression in *scrib* cells cannot be attributed to differences in transgene strength at the level of the Slit ligand. These data show that Robo2-Ena hyperactivation in *scrib* clones triggers tumorigenesis in the lumen following excess extrusion.

Slit-Robo2-Ena and JNK Form a Positive Feedback Loop

Given the dramatic effect of Slit-Robo2-Ena hyperactivation on the tumorigenic fate of *scrib* cells, we next investigated the effect of Slit-Robo2-Ena overexpression in normal cells. While plain Slit-overexpressing clones appeared normal (Figures 5A and S4M), Robo2- or Ena-overexpressing cells blocked from dying were extruded basally and accumulated F-actin (Figures 5B and 5C, quantified in Figure 5D). Without inhibiting cell death we could not observe these extruding cells (Figures S5A–S5D). As F-actin is linked to JNK activation (Uhlirova and Bohmann, 2006), we tested whether JNK was activated by Robo2-Ena overexpression. Indeed, cell-autonomous upregulation of the JNK-target MMP1 occurred in certain Robo2- or Ena-overexpressing cells (Figures 5E–5H', quantified in Figure S5Q), whereas Slit overexpression did not upregulate MMP1 (Figures S5E–S5F'). These data suggest that Robo2-Ena upregulation initiates a positive feedback loop between JNK and the Slit-Robo2-Ena module. Accordingly, *slit* transcription was also upregulated upon Robo2 overexpression (Figures 5I–5J') or Ena overexpression (Figures 5K–5L') in a JNK-dependent manner (Figures S5G–S5H'). Consistent with JNK upregulating the entire Slit-Robo2-Ena signaling module, Robo2 overexpression was sufficient to upregulate Ena (Figures S5I–S5J', quantified in Figure S5R), and Ena overexpression likewise upregulated Robo2 (Figures S5K–S5L', quantified in Figure S5R). Thus, activation of JNK or Robo2-Ena is sufficient to amplify and execute a cell-extrusion program. In contrast, Slit hyperactivation did not upregulate Robo2 or Ena (Figures S5M–S5P'). Slit's inability to initiate the positive feedback loop and amplify extrusive signaling may contribute to the infrequency of *scrib* luminal tumors upon Slit overexpression.

We further confirmed the positive feedback loop between JNK and Slit-Robo2-Ena by analyzing JNK-dependent cell death triggered by overexpression of the *Drosophila* tumor necrosis factor Eiger (Egr) in the eye (Igaki et al., 2002; Moreno et al., 2002). Significantly, JNK-dependent eye ablation was strongly suppressed by knockdown of Slit, Robo2, or Ena (Figures 5M–5Q, quantified in Figure 5R). Thus, JNK signaling is reinforced by a positive feedback loop with Slit-Robo2-Ena in a different cellular context.

E-Cadherin Disruption Extrudes Scrib Cells Downstream of Slit-Robo2-Ena

We next investigated the downstream mechanism of *scrib* cell extrusion. One attractive hypothesis is extrusion by deregulated E-cad (*Drosophila* homolog *shotgun*), especially as *scrib* cells were reported to have disrupted/downregulated E-cad (Pagliarini and Xu, 2003; Nakajima et al., 2013). Intriguingly, Slit-Robo hyperactivation disrupted E-cad-based adhesion in the *Drosophila* heart (Santiago-Martínez et al., 2008), and *robo2* mutant stem cell loss was partially rescued by E-cad overexpression (Stine et al., 2014). Moreover, Ena directly associates with adherens junctions in epithelia (Grevengoed et al., 2001), raising the possibility that Slit-Robo2-Ena extrudes cells through E-cad deregulation. Indeed, Robo2 or Ena overexpression triggered downregulation of junctional E-cad in extruding cells (Figures 6A–A'' and S6A–A'') and also caused sporadic ectopic E-cad in other cells. Consistent with a model in which disrupted E-cad triggers epithelial cell extrusion, *E-cad-RNAi* alone sufficed to extrude cells and activate JNK (Figures 6B–6C''). These data suggest that Robo2-Ena upregulation disrupts E-cad and cell adhesion to trigger extrusion.

We therefore hypothesized that *E-cad* disruption was required for *scrib* cell extrusion and death. Strikingly, E-cad overexpression in *scrib* cells strongly blocked extrusion and caused epithelial tumor overgrowth (Figures 6D–6G), phenocopying loss of Slit-Robo2-Ena in *scrib* clones. Notably, plain E-cad-overexpressing clones were actually smaller than control clones (Figures S6B–S6D), perhaps from β -catenin titration and altered Wingless signaling (Sanson et al., 1996). These data are consistent with Slit-Robo2-Ena activation disrupting cadherin-based adhesion to execute extrusion in *scrib* cells. A non-mutually exclusive hypothesis is that Ena-activated actomyosin generates an expulsive contractile force. Indeed, actomyosin strongly accumulated in *scrib*-overexpressing cells (Figures S6E–S6F'') as well as Robo2-overexpressing cells (Figures S6G–S6H''). Thus, both cadherin dysregulation and actomyosin changes may occur downstream of Slit-Robo2-Ena in evicting tumorigenic *scrib* cells by extrusion.

DISCUSSION

Here we show that JNK-activated Slit-Robo2-Ena signaling disrupts E-cad to extrude aberrant cells from epithelia. Slit-Robo2-Ena inactivation or E-cad overexpression in *scrib* clones caused epithelial tumors, while Robo2-Ena hyperactivation caused excess cell extrusion and luminal tumors (Figure 7A). Moreover, a positive feedback loop between JNK and Slit-Robo2-Ena likely ensures rapid commitment to cell extrusion and subsequent basal cell death (Figure 7B).

Slit-Robo and Ena signal through diverse mechanisms to affect cell mobility and adhesion (Reinhard et al., 2001; Krause et al., 2003; Ballard and Hinck, 2012). We found that Robo2

or Ena overexpression disrupted E-cad and extruded cells basally (Figures 5A–5D and 6A–6A’), consistent with Slit-Robo regulation of E-cad in different developmental and tumorigenic contexts (Santiago-Martínez et al., 2008; Zhou et al., 2011; Stine et al., 2014). An additional ramification of E-cad deregulation is increased cell scattering, as observed following Robo2 or Ena overexpression (Figures S4N and S4O; data not shown). Interestingly, increased cell mixing enhanced cell competition and elimination in the *Drosophila* pupal notum (Levayer et al., 2015). Thus, Slit-Robo’s disruption of E-cad may further facilitate *scrib* cell elimination by increased cell dispersion and exposure to wild-type cells. Alternatively, perturbation of adherens junctions could affect tumor growth by altering Hippo signaling (Yang et al., 2015).

Of the three Robo receptors, we found that only Robo2 is required for *scrib* cell elimination, which is intriguing given recent reports of non-canonical Slit-Robo2 signaling (e.g., Biteau and Jasper, 2014; Stine et al., 2014; Ordan and Volk, 2015; Evans et al., 2015). As Ena does not directly bind Robo2 (Bashaw et al., 2000) but can suppress Robo2-overexpression phenotypes (Bashaw et al., 2000; Simpson et al., 2000b), it is likely that the Robo2-Ena interaction is indirect, mediated perhaps by Abelson kinase (Abl; Bashaw et al., 2000).

JNK signaling drives dynamic cell movements during morphogenesis, including dorsal closure in *Drosophila* and neural tube and optic fissure in mice (Riesgo-Escovar et al., 1996; Xia and Karin, 2004). We identified a positive feedback loop between JNK and Slit-Robo2-Ena: JNK activation suffices to upregulate Slit-Robo2-Ena, and upregulation of Robo2 or Ena can activate JNK. Cadherin loss further solidifies this loop by activating JNK (Figure 6B). Future studies should determine whether Slit-Robo2-Ena signaling more broadly mediates cell movements downstream of JNK. Notably, Slit’s highly conserved human homolog (Slit2) and human Robo2 both possess human AP1 binding sites (ATGAGTCAT; three in Slit2 and nine in Robo2, data not shown), supporting that JNK-activated Slit-Robo could occur in mammals. Interestingly, in *scrib + Ras^{V12}* tumors, JNK upregulates the actin crosslinker Filamin/Cheerio to mediate metastasis (Külshammer and Uhlirova, 2013). Different JNK-activated actin regulators may therefore prevent or promote tumorigenesis depending on the tumor’s genetic context. Intriguingly, a recent study further connected JNK-dependent cell movement with axon-guidance genes: repulsive Semaphorin-Plexin signaling mediated epithelial wound repair, which is a dynamic and JNK-dependent process (Yoo et al., 2016). Thus, canonical “axon-guidance” signals may mediate manifold forms of cell-cell communication and movement.

Cell extrusion and cell competition are intimately linked to tissue homeostasis and tumor progression (Gu and Rosenblatt, 2012; Ballesteros-Arias et al., 2013; Enomoto et al., 2015), and the direction of cell extrusion can dictate whether a cancer is initiated or suppressed (Hogan et al., 2009; Slattum and Rosenblatt, 2014; Tamori et al., 2016). We also found that modulating extrusive signaling either promoted or suppressed *scrib* tumorigenesis (Figure 7): while plain Robo2 or Ena hyperactivation triggered basal epithelial cell extrusion followed by cell death (Figures 5B, 5C, and S4S–S4T’), Robo2-Ena activation in *scrib* mutant cells unexpectedly accelerated both basal and apical extrusion into the lumen (Figures 4G–4L). We speculate that the aberrant polarity of *scrib* cells permits a tumor-suppressive, basal cell-extrusion mechanism to deleteriously promote randomized cell

extrusion and luminal tumorigenesis. Indeed, luminal extrusion was recently identified as a causal mechanism of *scrib* tumorigenesis in the *Drosophila* wing disc (Tamori et al., 2016).

Notably, multiple human cancers are associated with dysregulated Slit-Robo signaling (reviewed in Ballard and Hinck, 2012). For example, human *slit2* was frequently silenced by promoter hypermethylation in breast and lung cancer cell lines (Dallol et al., 2002) as well as in 58% of breast cancer biopsies (Sharma et al., 2007). In addition, Robo2 and Slit were disrupted in human pancreatic cancers, with lower Robo2 associated with poor prognosis (Biankin et al., 2012). Importantly, however, Slit-Robo hyperactivation is also associated with human cancers. In a striking parallel to our findings, autocrine Slit-Robo overexpression degraded E-cadherin to promote epithelial-mesenchymal transition and tumor growth in human colorectal carcinoma lines (Zhou et al., 2011). Robo2 was also upregulated in various human hepatocellular carcinoma (HCC) lines (Avci et al., 2008), as was Ena (Hu et al., 2014); notably, HCC can invade the lumen of the bile duct (Carella et al., 1981). Moreover, upregulated Robo2 was linked to aggressive inflammatory breast cancer (Bieche et al., 2004), and Slit overexpression in pancreatic tumors triggered metastasis into lymphatic vessel lumens (Yang et al., 2010). The above findings are consistent with a model whereby gain of Slit-Robo2-Ena signaling exacerbates lumen tumorigenesis, but loss of Slit-Robo signaling prevents tumor cell elimination. Because *scrib* cell elimination also occurs in mammalian cell cultures (Norman et al., 2012), and given the conservation of Slit-Robo signaling in vertebrates (Araújo and Tear, 2003; Chisholm and Tessier-Lavigne, 1999), it may be fruitful to test whether dysregulated cell extrusion contributes to Slit-Robo's role in human tumorigenesis.

EXPERIMENTAL PROCEDURES

Fly Genetics

The following fly strains were used: *scrib*¹ (Bilder and Perrimon, 2000), *UAS-bsk*^{DN} (Adachi-Yamada et al., 1999b), *UAS-hep*^{CA} (Adachi-Yamada et al., 1999a), *UAS-eiger* (Igaki et al., 2002), *slit*² (Drosophila Genomics and Genetic Resources [DGGR] #106948), *robo1*^{GA285} (gift of Dietmar Schmucker), *slit*^{UC} (gift of Talila Volk), *slit-lacZ* (Bloomington #12189), *robo2*² (DGGR #106843), *robo2*¹ (Bloomington #34046), *robo3*¹ (gift of Talila Volk), *UAS-Robo2.HA* (gift of Talila Volk), *robo2*^{HA-robo2} (gift of Barry Dickson), *UAS-Slit* (gift of Tom Kidd), *UAS-comm* (gift of Tom Kidd), *UAS-sqh::mcherry/CyO* (Rauzi et al., 2010; gift of Kaoru Sugimura), *UAS-ena* (Bloomington #9139), *ena*²³ (Bloomington #8571), *Df(2R) Exel6069* (Bloomington #7551), *Df(2R)BSC349* (Bloomington #24373), *ena-RNAi* (Vienna Drosophila Resource Center [VDRC] #106484), *ena-RNAi*^{*} (VDRC #43056), *slit-RNAi* (VDRC #20210), *slit-RNAi*^{*} (Bloomington #31468), *robo2-RNAi* (Bloomington #9286), *robo2-RNAi*^{*} (Bloomington #27317), *robo1-RNAi* (VDRC #42441), *robo3-RNAi* (VDRC #44702), *shg-RNAi* (VDRC #27081), and *UAS-shg.DEFL* (DGGR #109004).

UAS-ena, *UAS-slit*, *UAS-robo2.HA*, and *UAS-robo2-RNAi* transgenes were recombined with *scrib*¹, FRT82B flies using neomycin to select for FRT82B and eye color to select for potential transgene-containing recombinants. The presence of both transgenes and *scrib*¹ was verified by complementation testing with *scrib*¹ and antibody counterstaining (i.e., anti-

Ena for UAS-ena recombinants). To monitor the stability of *scrib*¹ in subsequent experiments using these recombinants, we used phalloidin to label F-actin, which is drastically upregulated in *scrib* clones and thus permits unambiguous identification of *scrib* mutant cells. For *UAS-robo2.HA* and *UAS-robo2-RNAi* recombinations, multiple recombinant lines were isolated that phenocopied each other when expressed in *scrib* cells. *eyFLP5*, *Act>y+>GALA*, *UAS-GFP*, *FRT82B*, *tub-GAL80* generated MARCM, GFP⁺ clones mutant for *scrib* and/or driving *RNAi* (Lee and Luo, 1999). For all crosses, ten virgin females were mated to three males; all experiments were conducted at 25°C unless otherwise stated in the figure legends.

Immunohistochemistry

Wandering L3 larvae were dissected in 1% PBS and kept on ice until fixation in 4% paraformaldehyde (PFA) for 16 min. Following two washes in PBS and one in blocking agent (normal donkey serum), primary antibodies were applied overnight (8–12 hr, no rocking) in blocker + PBS + 1% Triton to allow tissue permeabilization. Following three washes in PBS, secondary antibodies were applied for 2.5 hr while rocking and covered (1:200). Samples were mounted with DAPI and 70% glycerol to provide volume. The following antibodies were used: rabbit anti-β-galactosidase for *slit-lacZ* (Sigma, 1:500), rabbit anti-cleaved *Drosophila* DCP1 (1:50, Cell Signaling Technology), mouse anti-Slit (Drosophila Studies Hybridoma Bank [DSHB], 1:500), mouse anti-Ena (DSHB, 1:500), rat anti-HA for *robo2^{HA}-Robo2* (Roche, 1:50), mouse anti-MMP1 (DSHB, 1:50), and Alexa647 phalloidin (1:25, Molecular Probes).

Data Acquisition and Analysis

For quantification of *scrib* clone size, representative cross-sections were analyzed in ImageJ, with total eye disc GFP clone area (selected by thresholding for GFP, with parameters kept consistent across all genetic backgrounds) divided by total eye disc area (selected by hand). We excluded the antennal disc from analysis as *scrib* cells are less robustly eliminated in antennal discs. For antibody quantification within clones or wild-type cells, a minimum of three eye discs was analyzed in ImageJ for the mean signal intensity of GFP clones versus neighboring wild-type cells. For quantifying localization of *scrib* clones, z-stack data from a minimum of five eye discs stained with phalloidin and/or DAPI was acquired at 1-μm intervals on an SP8-upright Leica confocal microscope and then analyzed by eye using Leica software and ImageJ. For quantification of Eiger-induced eye ablation, the eye area of female flies was measured manually in ImageJ and then normalized to *GMR-GAL4* eye area. Data were plotted in R (version 3.2.2). Excel was used to conduct two-tailed Student's t tests for statistical analyses (*p<0.05, **p<0.01, ***p<0.001, ****p<0.0001).

Supplementary Material

Refer to Web version on PubMed Central for supplementary material.

ACKNOWLEDGMENTS

The authors thank Daisuke Kizawa for pioneering the initial deficiency screen; Kanako Baba, Shio Sekizawa, and Akiko Sogo for technical support; Masatoshi Yamamoto, Chiaki Iida, Yuya Sanaki, Masato Enomoto, and Elly

Ordan for fruitful discussions, advice, and sharing unpublished data; Mai Nakamura and Jenelle Lee for assistance with diagrams; Tom Kidd, Barry Dickson, Dietmar Schmucker, Talila Volk, and Kaoru Sugimura for kindly sharing fly stocks; anonymous reviewers for helpful insight; the Developmental Studies Hybrid-oma Bank (Iowa City, IA, USA) for antibodies; and the Bloomington *Drosophila* Stock Center (Indiana, USA), the Vienna *Drosophila* Resource Center (Vienna, Austria), and the *Drosophila* Genomics and Genetic Resources (Kyoto Stock Center, Japan) for fly stocks. This work was supported by grants from the Ministry of Education, Culture, Sports, Science and Technology (MEXT) to J.V. and T.I., Grant-in-Aid for Scientific Research (A) (Grant No. 16H02505) to T.I., Grant-in-Aid for Scientific Research on Innovative Areas (Grant No. 26114002) to T.I., the Naito Foundation to T.I., the Takeda Science Foundation to T.I., and the Japan Science and Technology Agency to T.I.

REFERENCES

- Adachi-Yamada T, Fujimura-Kamada K, Nishida Y, and Matsumoto K (1999a). Distortion of proximodistal information causes JNK-dependent apoptosis in *Drosophila* wing. *Nature* 400, 166–169. [PubMed: 10408443]
- Adachi-Yamada T, Gotoh T, Sugimura I, Tateno M, Nishida Y, Onuki T, and Date H (1999b). De novo synthesis of sphingolipids is required for cell survival by down-regulating c-Jun N-terminal kinase in *Drosophila* imaginal discs. *Mol. Cell. Biol* 19, 7276–7286. [PubMed: 10490662]
- Ahern-Djamali SM, Comer AR, Bachmann C, Kastenmeier AS, Reddy SK, Beckerle MC, Walter U, and Hoffmann FM (1998). Mutations in *Drosophila* enabled and rescue by human vasodilator-stimulated phosphoprotein (VASP) indicate important functional roles for Ena/VASP homology domain 1 (EVH1) and EVH2 domains. *Mol. Biol. Cell* 9, 2157–2171. [PubMed: 9693373]
- Amoyel M, and Bach EA (2014). Cell competition: how to eliminate your neighbours. *Development* 141, 988–1000. [PubMed: 24550108]
- Angel P, Imagawa M, Chiu R, Stein B, Imbra RJ, Rahmsdorf HJ, Jonat C, Herrlich P, and Karin M (1987). Phorbol ester-inducible genes contain a common *cis* element recognized by a TPA-modulated *trans*-acting factor. *Cell* 49, 729–739. [PubMed: 3034432]
- Araújo SJ, and Tear G (2003). Axon guidance mechanisms and molecules: lessons from invertebrates. *Nat. Rev. Neurosci* 4, 910–922. [PubMed: 14595402]
- Avcı ME, Konu O, and Yagci T (2008). Quantification of SLIT-ROBO transcripts in hepatocellular carcinoma reveals two groups of genes with coordinate expression. *BMC Cancer* 8, 392. [PubMed: 19114000]
- Ballard MS, and Hinck L (2012). A roundabout way to cancer. *Adv. Cancer Res.* 114, 187–235. [PubMed: 22588058]
- Ballesteros-Arias L, Saavedra V, and Morata G (2013). Cell competition may function either as tumour-suppressing or as tumour-stimulating factor in *Drosophila*. *Oncogene* 33, 4377–4384. [PubMed: 24096487]
- Bashaw GJ, Kidd T, Murray D, Pawson T, and Goodman CS (2000). Repulsive axon guidance: Abelson and Enabled play opposing roles downstream of the roundabout receptor. *Cell* 101, 703–715. [PubMed: 10892742]
- Biankin AV, Waddell N, Kassahn KS, Gingras MC, Muthuswamy LB, Johns AL, Miller DK, Wilson PJ, Patch AM, Wu J, et al. (2012). Pancreatic cancer genomes reveal aberrations in axon guidance pathway genes. *Nature* 491, 399–405. [PubMed: 23103869]
- Bieche I, Lerebours F, Tozlu S, Espie M, Marty M, and Lidereau R (2004). Molecular profiling of inflammatory breast cancer: identification of a poor-prognosis gene expression signature. *Clin. Cancer Res.* 10, 6789–6795. [PubMed: 15501955]
- Bilder D, and Perrimon N (2000). Localization of apical epithelial determinants by the basolateral PDZ protein Scribble. *Nature* 403, 676–680. [PubMed: 10688207]
- Biteau B, and Jasper H (2014). Slit/Robo signaling regulates cell fate decisions in the intestinal stem cell lineage of *Drosophila*. *Cell Rep.* 7, 1867–1875. [PubMed: 24931602]
- Brose K, and Tessier-Lavigne M (2000). Slit proteins: key regulators of axon guidance, axonal branching, and cell migration. *Curr. Opin. Neurobiol* 10, 95–102. [PubMed: 10679444]
- Brose K, Bland KS, Wang KH, Arnott D, Henzel W, Goodman CS, Tessier-Lavigne M, and Kidd T (1999). Slit proteins bind Robo receptors and have an evolutionarily conserved role in repulsive axon guidance. *Cell* 96, 795–806. [PubMed: 10102268]

- Brumby AM, and Richardson HE (2003). Scribble mutants cooperate with oncogenic Ras or Notch to cause neoplastic overgrowth in *Drosophila*. *EMBO J.* 22, 5769–5779. [PubMed: 14592975]
- Carella G, Degott C, and Benhamou JP (1981). Invasion of the lumen of the bile ducts by hepatocellular carcinoma. *Liver* 1, 251–254. [PubMed: 6294440]
- Chisholm A, and Tessier-Lavigne M (1999). Conservation and divergence of axon guidance mechanisms. *Curr. Opin. Neurobiol* 9, 603–615. [PubMed: 10508749]
- Dallol A, Da Silva NF, Viacava P, Minna JD, Bieche I, Maher ER, and Latif F (2002). SLIT2, a human homologue of the *Drosophila* Slit2 gene, has tumor suppressor activity and is frequently inactivated in lung and breast cancers. *Cancer Res.* 62, 5874–5880. [PubMed: 12384551]
- de Beco S, Ziosi M, and Johnston LA (2012). New frontiers in cell competition. *Dev. Dyn* 241, 831–841. [PubMed: 22438309]
- Domyan ET, Branchfield K, Gibson DA, Naiche LA, Lewandoski M, Tessier-Lavigne M, Ma Le, and Sun X (2013). Roundabout receptors are critical for foregut separation from the body wall. *Dev. Cell* 24, 52–63. [PubMed: 23328398]
- Enomoto M, Vaughen J, and Igaki T (2015). Non-autonomous overgrowth by oncogenic niche cells: cellular cooperation and competition in tumorigenesis. *Cancer Sci.* 106, 1651–1658. [PubMed: 26362609]
- Evans TA, Santiago C, Arbeille E, and Bashaw GJ (2015). Robo2 acts in trans to inhibit Slit-Robo1 repulsion in pre-crossing commissural axons. *Elife* 4, e08407. [PubMed: 26186094]
- Gu Y, and Rosenblatt J (2012). New emerging roles for epithelial cell extrusion. *Curr. Opin. Cell Biol.* 24, 865–870. [PubMed: 23044222]
- Grevengoed EE, Loureiro JJ, Jesse TL, and Peifer M (2001). Abelson kinase regulates epithelial morphogenesis in *Drosophila*. *J. Cell Biol.* 155, 1185–1198. [PubMed: 11756472]
- Hogan C, Dupré-Crochet S, Norman M, Kajita M, Zimmermann C, Pelling AE, Piddini E, Baena-López LA, Vincent J-P, Itoh Y, et al. (2009). Characterization of the interface between normal and transformed epithelial cells. *Nat. Cell Biol.* 11, 460–467. [PubMed: 19287376]
- Hu K, Wang J, Yao Z, Liu B, Lin Y, Liu L, and Xu L (2014). Expression of cytoskeleton regulatory protein Mena in human hepatocellular carcinoma and its prognostic significance. *Med. Oncol* 31, 939–947. [PubMed: 24683008]
- Igaki T, Kanda H, Yamamoto-Goto Y, Kanuka H, Kuranaga E, Aigaki T, and Miura M (2002). Eiger, a TNF superfamily ligand that triggers the *Drosophila* JNK pathway. *EMBO J.* 21, 3009–3018. [PubMed: 12065414]
- Igaki T, Pastor-Pareja JC, Aonuma H, Miura M, and Xu T (2009). Intrinsic tumor suppression and epithelial maintenance by endocytic activation of Eiger/TNF signaling in *Drosophila*. *Dev. Cell* 16, 458–465. [PubMed: 19289090]
- Keleman K, Rajagopalan S, Cleppien D, Teis D, Paiha K, Huber LA, Technau GM, and Dickson BJ (2002). Comm sorts robo to control axon guidance at the *Drosophila* midline. *Cell* 110, 415–427. [PubMed: 12202032]
- Kidd T, Bland KS, and Goodman CS (1999). Slit is the midline repellent for the robo receptor in *Drosophila*. *Cell* 96, 785–794. [PubMed: 10102267]
- Krause M, Dent EW, Bear JE, Loureiro JJ, and Gertler FB (2003). Ena/VASP proteins: regulators of the actin cytoskeleton and cell migration. *Annu. Rev. Cell Dev. Biol* 19, 541–564. [PubMed: 14570581]
- Külshammer E, and Uhlirova M (2013). The actin cross-linker Filamin/Cheerio mediates tumor malignancy downstream of JNK signaling. *J. Cell Sci.* 126, 927–938. [PubMed: 23239028]
- Lee T, and Luo L (1999). Mosaic analysis with a repressible cell marker for studies of gene function in neuronal morphogenesis. *Neuron* 22, 451–461. [PubMed: 10197526]
- Levayer R, and Moreno E (2013). Mechanisms of cell competition: themes and variations. *J. Cell Biol.* 200, 689–698. [PubMed: 23509066]
- Levayer R, Hauert B, and Moreno E (2015). Cell mixing induced by myc is required for competitive tissue invasion and destruction. *Nature* 524, 476–480. [PubMed: 26287461]
- Levayer R, Dupont C, and Moreno E (2016). Tissue crowding induces caspase-dependent competition for space. *Curr. Biol* 26, 670–677. [PubMed: 26898471]

- Lolo F-N, Casas-Tinto S, and Moreno E (2012). Cell competition time line: winners kill losers, which are extruded and engulfed by hemocytes. *Cell Rep.* 2, 526–539. [PubMed: 22981235]
- Morata G, and Ballesteros-Arias L (2015). Cell competition, apoptosis and tumour development. *Int. J. Dev. Biol* 59, 79–86. [PubMed: 26374529]
- Moreno E, Yan M, and Basler K (2002). Evolution of TNF signaling mechanisms: JNK-dependent apoptosis triggered by Eiger, the *Drosophila* homolog of the TNF superfamily. *Curr. Biol* 12, 1263–1268. [PubMed: 12176339]
- Nakajima Y-I, Meyer EJ, Kroesen A, McKinney SA, and Gibson MC (2013). Epithelial junctions maintain tissue architecture by directing planar spindle orientation. *Nature* 500, 359–362. [PubMed: 23873041]
- Norman M, Wisniewska KA, Lawrenson K, Garcia-Miranda P, Tada M, Kajita M, Mano H, Ishikawa S, Ikegawa M, Shimada T, et al. (2012). Loss of Scribble causes cell competition in mammalian cells. *J. Cell Sci.* 125, 59–66. [PubMed: 22250205]
- Ohsawa S, Sugimura K, Takino K, Xu T, Miyawaki A, and Igaki T (2011). Elimination of oncogenic neighbors by JNK-mediated engulfment in *Drosophila*. *Dev. Cell* 20, 315–328. [PubMed: 21397843]
- Ordan E, and Volk T (2015). A non-signaling role of Robo2 in tendons is essential for Slit processing and muscle patterning. *Development* 142, 3512–3518. [PubMed: 26400093]
- Pagliarini RA, and Xu T (2003). A genetic screen in *Drosophila* for metastatic behavior. *Science* 302, 1227–1231. [PubMed: 14551319]
- Rajagopalan S, Vivancos V, Nicolas E, and Dickson BJ (2000). Selecting a longitudinal pathway: robo receptors specify the lateral position of axons in the *Drosophila* CNS. *Cell* 103, 1033–1045. [PubMed: 11163180]
- Rauzi M, Lenne P-F, and Lecuit T (2010). Planar polarized actomyosin contractile flows control epithelial junction remodelling. *Nature* 468, 1110–1114. [PubMed: 21068726]
- Reinhard M, Jarchau T, and Walter U (2001). Actin-based motility: stop and go with Ena/VASP proteins. *Trends Biochem. Sci* 26, 243–249. [PubMed: 11295557]
- Riesgo-Escovar JR, Jenni M, Fritz A, and Hafen E (1996). The *Drosophila* Jun-N-terminal kinase is required for cell morphogenesis but not for DJun-dependent cell fate specification in the eye. *Genes Dev.* 10, 2759–2768. [PubMed: 8946916]
- Sanson B, White P, and Vincent JP (1996). Uncoupling cadherin-based adhesion from wingless signalling in *Drosophila*. *Nature* 383, 627–630. [PubMed: 8857539]
- Santiago-Martínez E, Soplóp NH, Patel R, and Kramer SG (2008). Repulsion by Slit and Roundabout prevents Shotgun/E-cadherin-mediated cell adhesion during *Drosophila* heart tube lumen formation. *J. Cell Biol.* 182, 241–248. [PubMed: 18663139]
- Sharma G, Mirza S, Prasad CP, Srivastava A, Gupta SD, and Ralhan R (2007). Promoter hypermethylation of p16INK4A, p14ARF, CyclinD2 and Slit2 in serum and tumor DNA from breast cancer patients. *Life Sci.* 80, 1873–1881. [PubMed: 17383681]
- Simpson JH, Bland KS, Fetter RD, and Goodman CS (2000a). Short-range and long-range guidance by Slit and its Robo receptors: a combinatorial code of Robo receptors controls lateral position. *Cell* 103, 1019–1032. [PubMed: 11163179]
- Simpson JH, Kidd T, Bland KS, and Goodman CS (2000b). Short-range and long-range guidance by slit and its Robo receptors. Robo and Robo2 play distinct roles in midline guidance. *Neuron* 28, 753–766. [PubMed: 11163264]
- Slattum GM, and Rosenblatt J (2014). Tumour cell invasion: an emerging role for basal epithelial cell extrusion. *Nat. Rev. Cancer* 14, 495–501. [PubMed: 24943812]
- Spitzweck B, Brankatschk M, and Dickson BJ (2010). Distinct protein domains and expression patterns confer divergent axon guidance functions for *Drosophila* robo receptors. *Cell* 140, 409–420. [PubMed: 20144763]
- Stine RR, Greenspan LJ, Ramachandran KV, and Matunis EL (2014). Coordinate regulation of stem cell competition by slit-robo and JAK-STAT signaling in the *Drosophila* testis. *PLoS Genet.* 10, e1004713. [PubMed: 25375180]
- Stowers RS, and Schwarz TL (1999). A genetic method for generating *Drosophila* eyes composed exclusively of mitotic clones of a single genotype. *Genetics* 152, 1631–1639. [PubMed: 10430588]

- Tamori Y, and Deng W-M (2011). Cell competition and its implications for development and cancer. *J. Genet. Genomics* 38, 483–495. [PubMed: 22035869]
- Tamori Y, Suzuki E, and Deng W-M (2016). Epithelial tumors originate in tumor hotspots, a tissue-intrinsic microenvironment. *PLoS Biol.* 14, e1002537. [PubMed: 27584724]
- Uhlirova M, and Bohmann D (2006). JNK- and Fos-regulated Mmp1 expression cooperates with Ras to induce invasive tumors in *Drosophila*. *EMBO J.* 25, 5294–5304. [PubMed: 17082773]
- Xia Y, and Karin M (2004). The control of cell motility and epithelial morpho-genesis by Jun kinases. *Trends Cell Biol.* 14, 94–101. [PubMed: 15102441]
- Yang X-M, Han H-X, Sui F, Dai Y-M, Chen M, and Geng J-G (2010). Slit-Robo signaling mediates lymphangiogenesis and promotes tumor lymphatic metastasis. *Biochem. Biophys. Res. Commun.* 396, 571–577. [PubMed: 20438712]
- Yang C-C, Graves HK, Moya IM, Tao C, Hamaratoglu F, Gladden AB, and Halder G (2015). Differential regulation of the Hippo pathway by adherens junctions and apical-basal cell polarity modules. *Proc. Natl. Acad. Sci. USA* 112, 1785–1790. [PubMed: 25624491]
- Yoo SK, Pascoe HG, Pereira T, Kondo S, Jacinto A, Zhang X, and Hariharan IK (2016). Plexins function in epithelial repair in both *Drosophila* and zebrafish. *Nat. Commun* 7, 1–12.
- Yu TW, Hao JC, Lim W, Tessier-Lavigne M, and Bargmann CI (2002). Shared receptors in axon guidance: SAX-3/Robo signals via UNC-34/Enabled and a Netrin-independent UNC-40/DCC function. *Nat. Neurosci* 5, 1147–1154. [PubMed: 12379860]
- Zhou W-J, Geng ZH, Chi S, Zhang W, Niu X-F, Lan S-J, Ma L, Yang X, Wang L-J, Ding Y-Q, et al. (2011). Slit-Robo signaling induces malignant transformation through Hakai-mediated E-cadherin degradation during colorectal epithelial cell carcinogenesis. *Cell Sci.* 21, 609–626.

Highlights

- Autocrine Slit-Robo2-Ena signaling eliminates tumorigenic epithelial cells
- Slit-Robo2-Ena extrudes polarity-deficient cells by disrupting E-cadherin
- Robo2-Ena hyperactivation triggers excess extrusion and luminal tumorigenesis
- A positive feedback loop between JNK and Robo2-Ena amplifies extrusive signaling

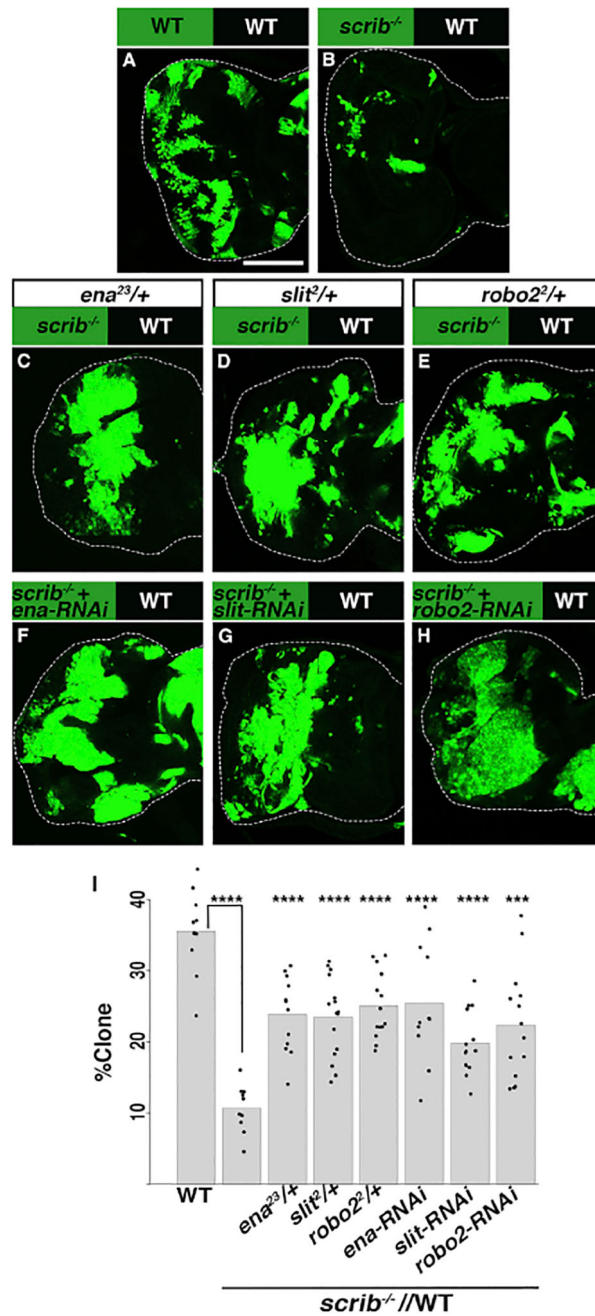


Figure 1. Slit-Robo2-Ena Are Required for *scrib* Elimination

(A–H) Wild-type (WT) GFP clones (A) contribute significantly more to eye disc tissue than *scrib* clones, which are eliminated (B; eye disc is outlined and posterior is to the left in all images). Heterozygosity for *ena* (C), *slit* (D), or *robo2* (E) potentiated *scrib* cell overgrowth, as did *RNAi* expressed inside *scrib* against *ena* (F), *slit* (G), or *robo2* (H). Scale bar, 100 μ m. (I) Quantification of clone size by % GFP area/disc. Statistical significance is assessed against plain *scrib* (bar #2) in all graphs unless otherwise indicated. *** $p < 0.001$, **** $p < 0.0001$.

See Experimental Procedures and Supplemental Experimental Procedures for detailed genotypes and quantification methodology, and Figure S1 for related experiments.

Author Manuscript

Author Manuscript

Author Manuscript

Author Manuscript

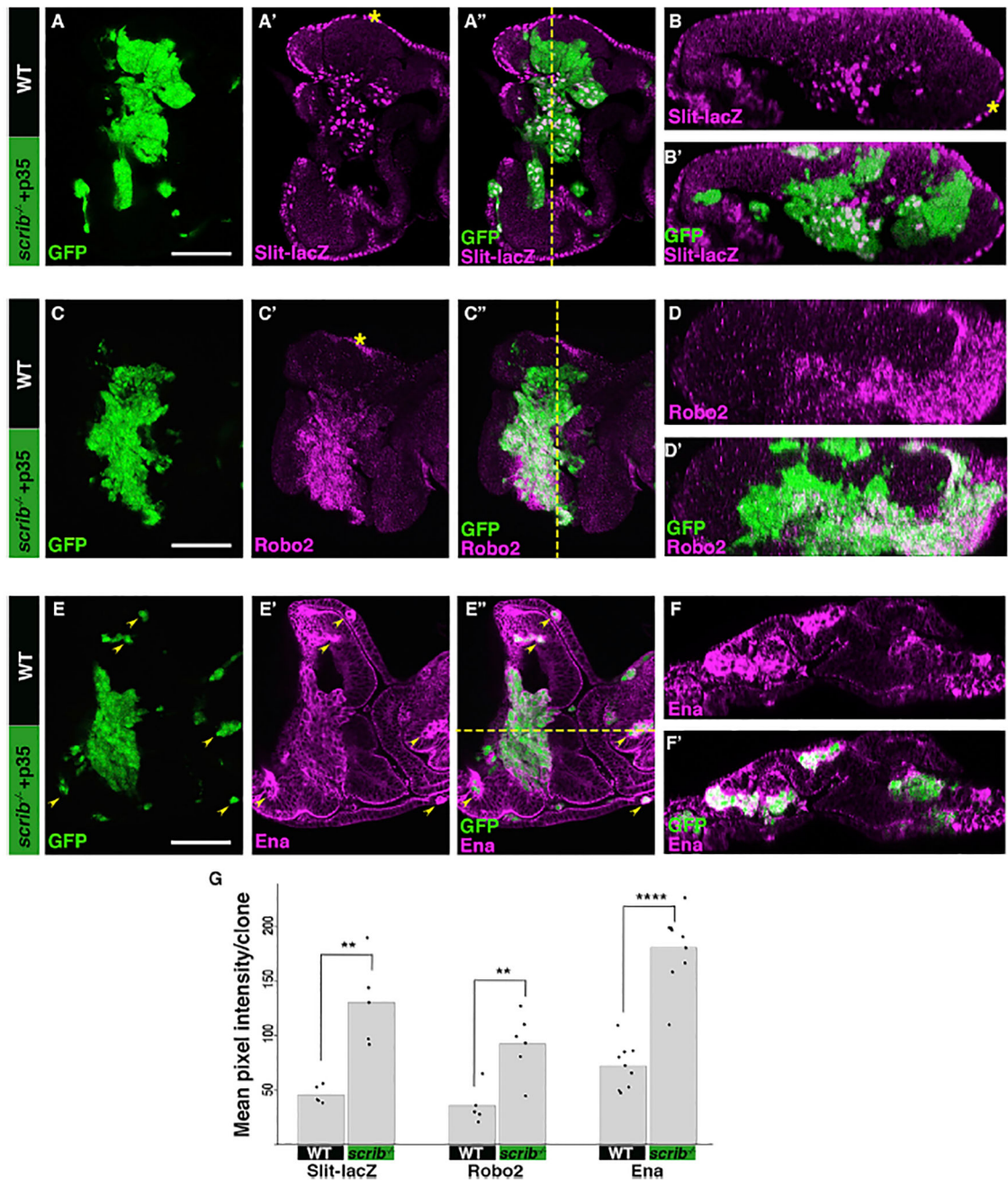


Figure 2. Slit-Robo2-Ena Are Upregulated Inside *scrib* Cells

(A–F') *scrib* clones co-expressing caspase inhibitor p35 were stained for *slit-lacZ* (A–B'); asterisk marks endogenous expression in all images), Robo2 (C–D'), or Ena (E–F', arrowheads point to cell-autonomous accumulation inside *scrib* clones). Dashed lines indicate xz or yz sections shown adjacent to cross-sections. Scale bars, 100 μ m.

(G) Quantification of *slit-lacZ*, Robo2, and Ena in *scrib* cells versus neighboring wild-type cells.

See Experimental Procedures and Supplemental Information for detailed genotypes and antibody staining and Figure S2 for related experiments. ** $p < 0.01$, **** $p < 0.0001$.

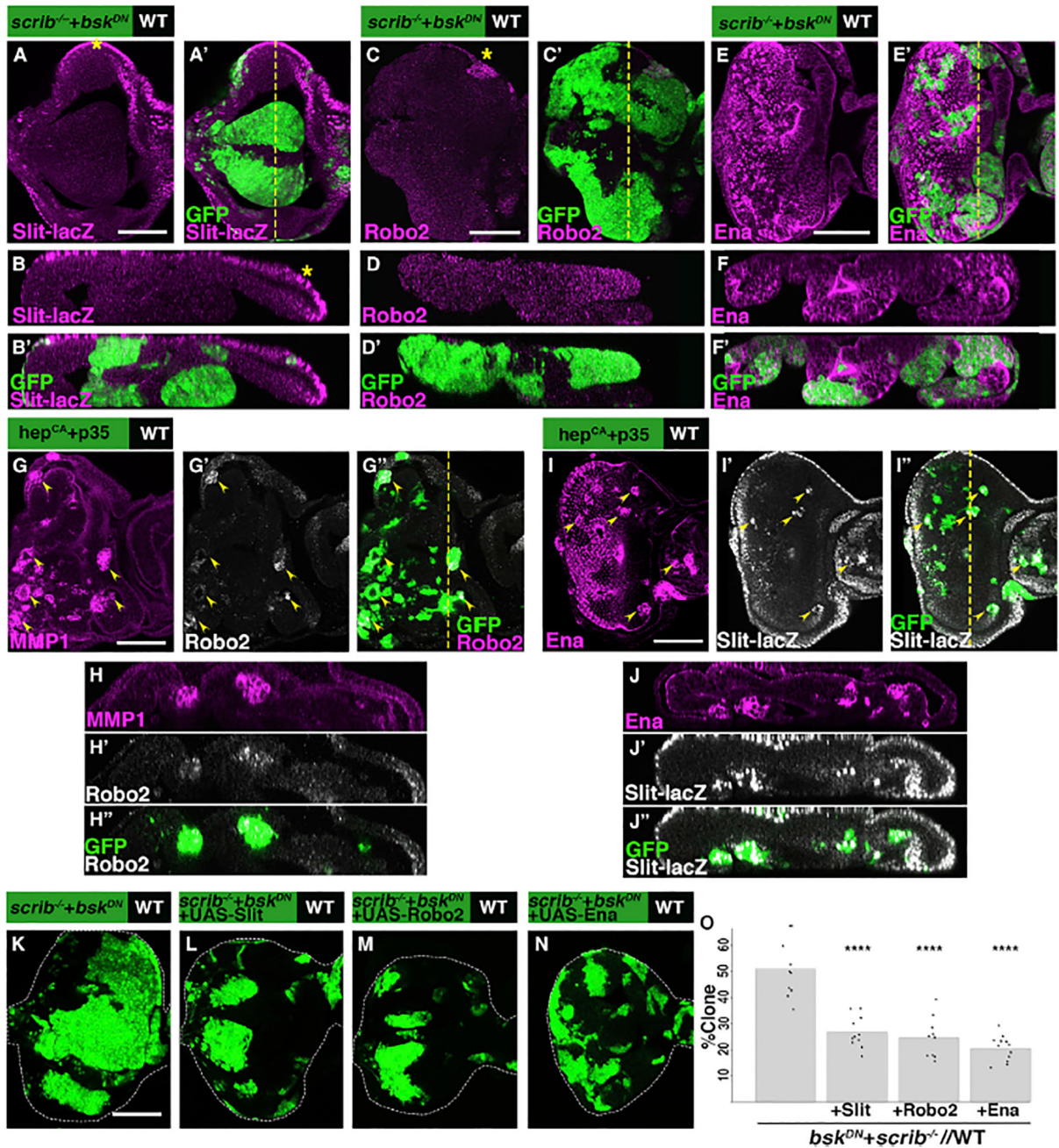


Figure 3. Slit-Robo2-Ena Act Downstream of JNK Signaling in *scrib* Cell Elimination
 (A–F) Blocking JNK signaling in *scrib* clones (+*bsk*^{DN}) abolished upregulation of *slit-lacZ* (A–B'; asterisk marks endogenous), Robo2 (C–D'), or Ena (E–F', note lack of cell-autonomous accumulation as shown in Figures 2E–2F').
 (G–J) Conversely, JNK activation (*hep*^{CA} + *p35*) triggered cell-autonomous Robo2 accumulation (arrowheads G'–G'', H'–H''); MMP1 is positive control [G, H]), *slit-lacZ* upregulation (arrowheads I'–I'', J'–J''), and Ena accumulation (I, J).

(K–O) While JNK-impaired *scrib* clones massively overgrow (K), overexpressing Slit (L), Robo2 (M), or Ena (N) significantly rescued overgrowth (quantified in O, significance measured against *scrib + bsk^{DN}* [bar #1]). ****p < 0.0001. Scale bars, 100 μ m. See Supplemental Information for detailed genotypes and Figure S3 for related experiments.

Author Manuscript

Author Manuscript

Author Manuscript

Author Manuscript

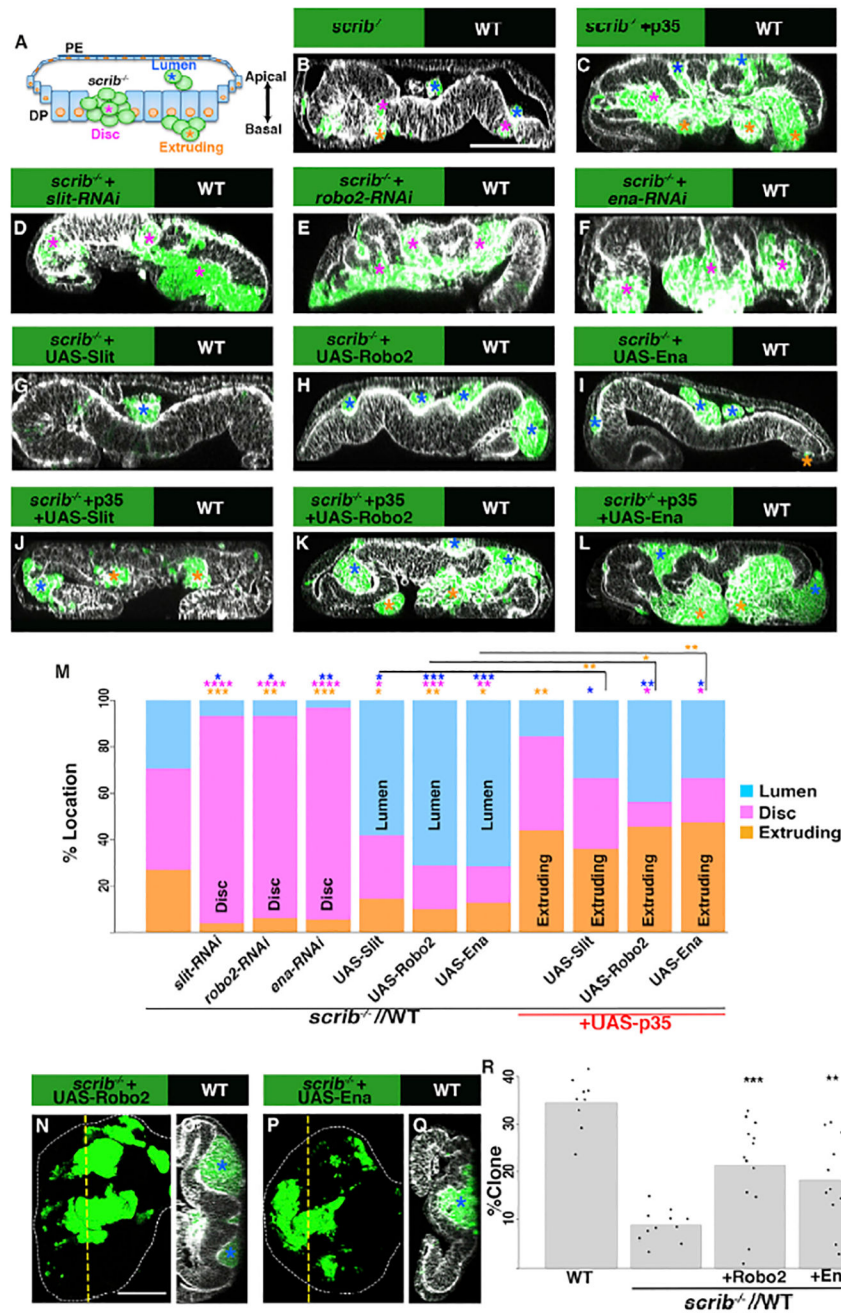


Figure 4. Slit-Robo2-Ena Extrude *scrib* Cells, and Robo2-Ena Hyperactivation Promotes *scrib* Lumen Tumorigenesis
 (A–M) Schematic (A) of an eye disc harboring *scrib* cells (green): the main epithelium (disc proper, DP) is encased by a thin peripodial epithelium (PE), forming a lumen that contacts apical cell surfaces. *scrib* cells are either within the DP (“Disc,” magenta asterisk), extruding basally (“Extruding,” orange asterisk), or in the lumen (“Lumen,” blue asterisk), as shown in (B) with F-actin labeled in white. Blocking death in *scrib* cells (+*p35*) revealed many basally extruding cells (C, orange asterisk). Impairing *slit* (D), *robo2* (E), or *ena* (F) within *scrib* by *RNAi* blocked cell extrusion (magenta asterisk). Strikingly, overexpressing Slit (G), Robo2

(H), or Ena (I) in *scrib* cleared most *scrib* cells from the DP, with remaining cells mainly located in the lumen (blue asterisk). Blocking cell death in Slit-Robo2-Ena over-expression *scrib* clones again revealed many basally extruding cells (J–L, orange asterisk). (M) Quantification of *scrib* clone location (Extruding, Disc, or Lumen) as percentage of total *scrib* area (n = minimum of 5 discs/genotype). Statistical significance coloring (*p < 0.05, **p < 0.01, ***p < 0.001, ****p < 0.0001) corresponds to clone location; bars #2–8, significance measured against bar #1, plain *scrib*; bars #9–11, significance measured against bar #8, *scrib* + *p35*.

(N–R) Robo2 (N and O) or Ena hyperactivation (P and Q) in *scrib* cells triggered lumen tumor formation (quantified in R, WT represents plain GFP clones; **p < 0.01, ***p < 0.001).

Scale bars, 100 μ m. See Supplemental Information for detailed genotypes and Figure S4 for related experiments.

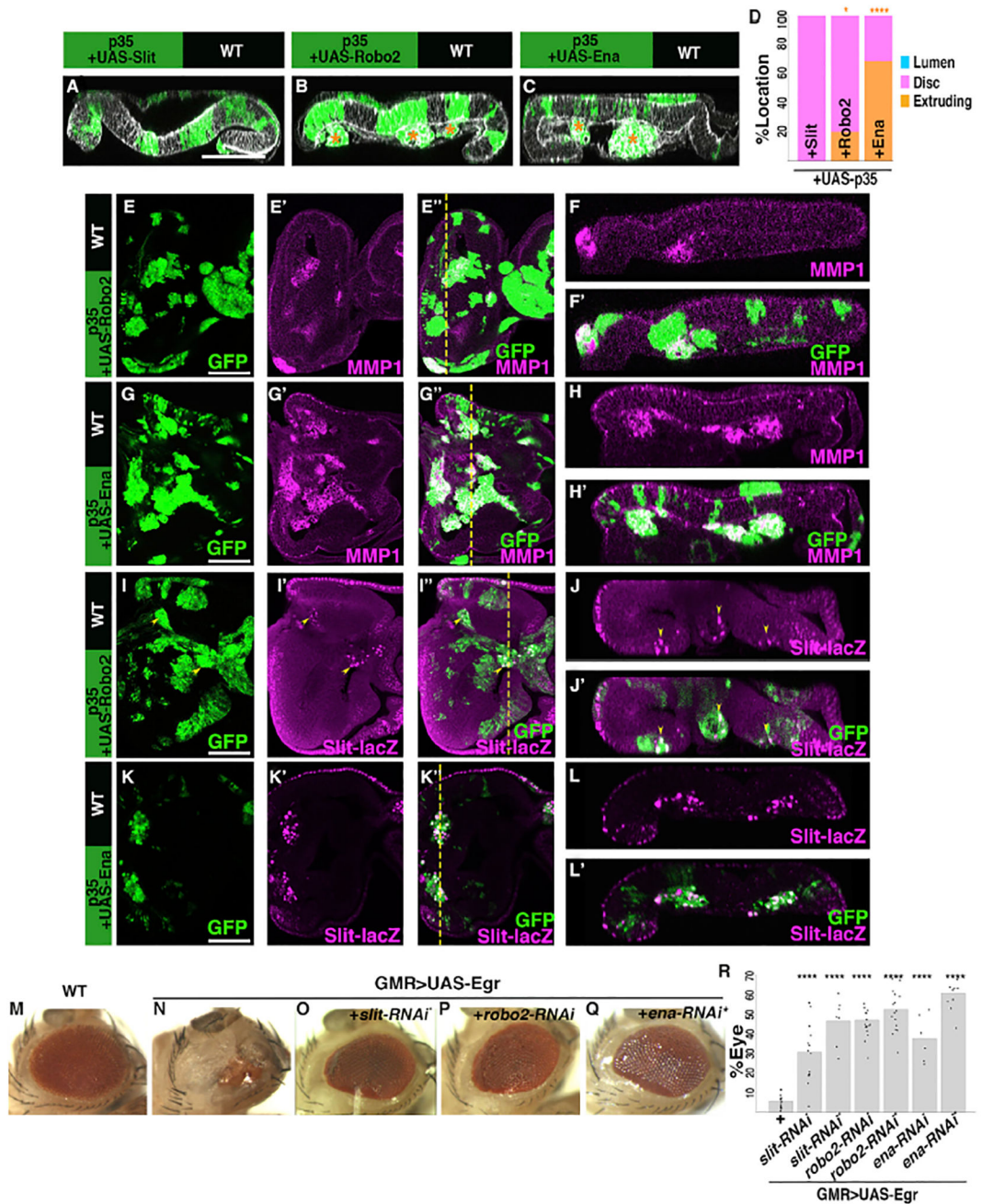


Figure 5. Slit-Robo2-Ena and JNK Form a Positive Feedback Loop

(A–D) Slit-overexpressing clones (A) appeared wild-type, whereas Robo2 (B) or Ena-overexpressing clones (C) extruded basally and accumulated F-actin (orange asterisk, quantified in D). (E–L) Plain Robo2 hyperactivation (E–F') or Ena hyperactivation (G–H') caused cell-autonomous JNK activation, as assessed by MMP1. Accordingly, Robo2 hyperactivation (arrowheads I–J') or Ena hyperactivation (K–L') could therefore upregulate *slit-lacZ*.

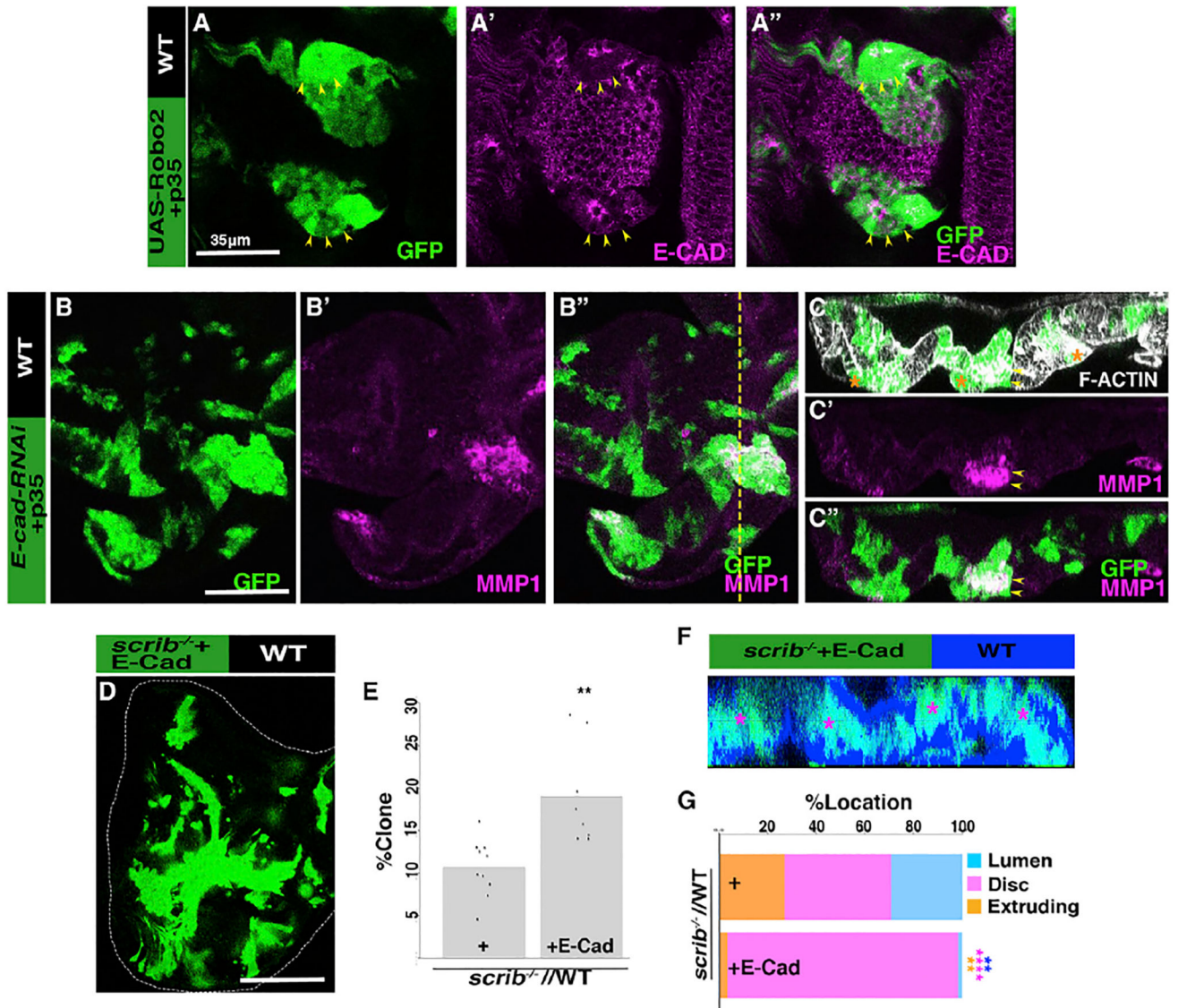
(M–R) While Eiger (Egr) overexpression by *GMR-GAL4* ablates adult eyes (N, compare with M), co-expression of *slit-RNAi** (O), *robo2-RNAi* (P), or *ena-RNAi** (Q) rescued eye ablation. (R) Quantification of eye size normalized to *GMR-GAL4* eyes. ****p < 0.0001. Scale bars, 100 μ m. See Supplemental Experimental Procedures for detailed genotypes and Figure S5 for related experiments.

Author Manuscript

Author Manuscript

Author Manuscript

Author Manuscript



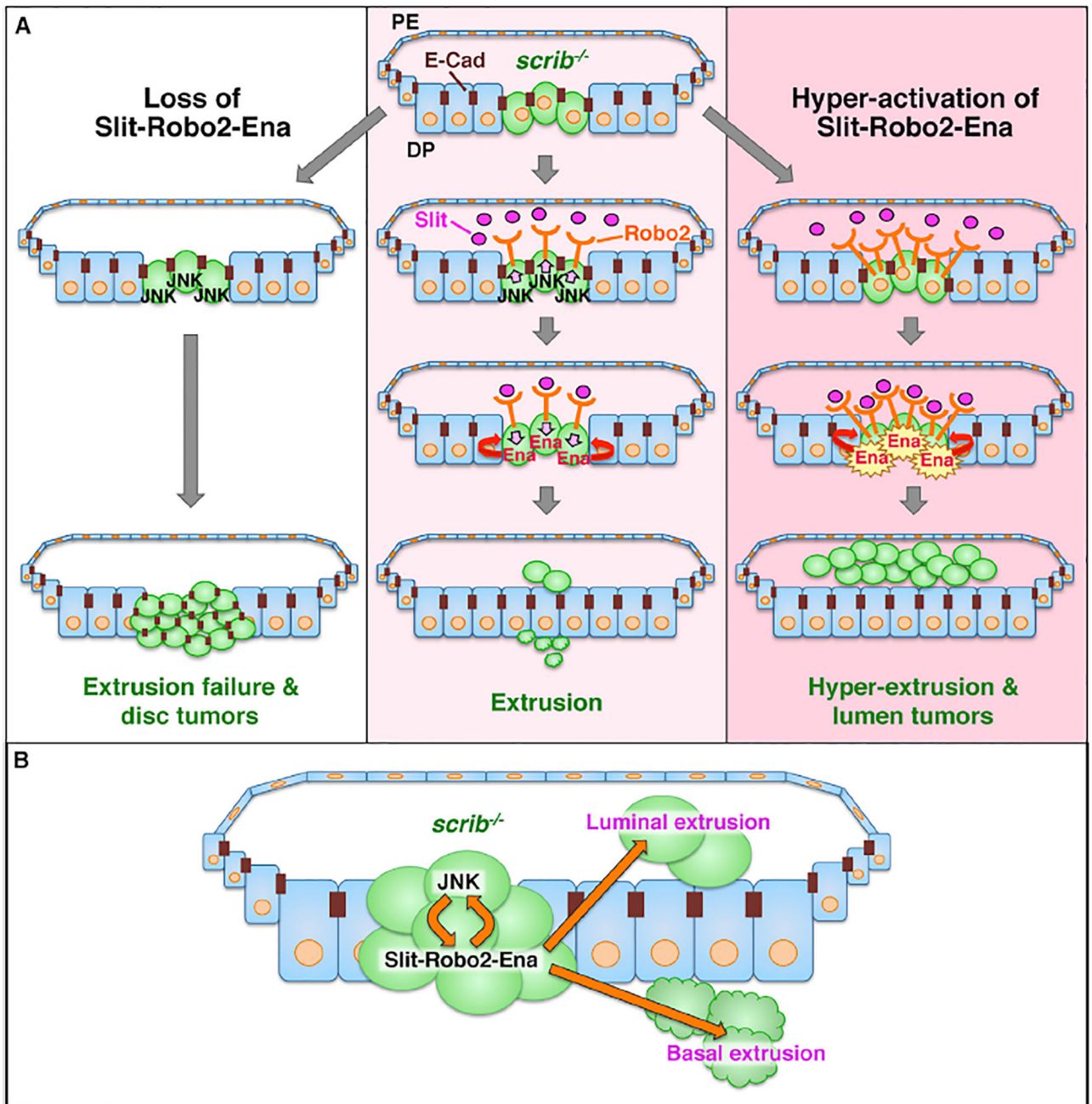


Figure 7. Model for Slit-Robo2-Ena Regulation of *scrib* Tumorigenesis

(A) Inactivation of Slit-Robo2-Ena causes *scrib* cell overgrowth in the main epithelial disc (disc proper, DP), whereas normally JNK-activated Slit-Robo2-Ena extrudes *scrib* cells by E-cad disruption and subsequent basal cell death. Conversely, hyperactivation of Robo2-Ena triggers excess extrusion and luminal tumor overgrowth between the DP and the peripodial epithelium (PE).

(B) JNK and Slit-Robo2-Ena form a positive feedback loop in *scrib* that rapidly extrudes *scrib* cells.